Ultrastructural Immunolocalization of Arabinogalactan Protein, Pectin and Hemicellulose Epitopes Through Anther Development in *Brassica napus*

Running head: Cell wall changes during *B. napus* anther development

Corresponding author:

Prof. J.M. Seguí-Simarro.

COMAV - Universitat Politècnica de València. CPI, Edificio 8E - Escalera I, Camino de Vera, s/n, 46022. Valencia, Spain.

Tel/Fax: +34963879047. e-mail: seguisim@btc.upv.es

Subject areas:

(1) Growth and development

(6) structure and function of cells

Number of black and white figures: 8

Number of color figures: 0

Number of tables: 1

Type and number of supplementary material: 3 figures grouped in a single pdf file

Ultrastructural immunolocalization of arabinogalactan protein, pectin and hemicellulose epitopes through anther development in *Brassica napus*

Running head: Cell wall changes during *B. napus* anther development

Patricia Corral-Martínez[1], Edgar García-Fortea[1], Sophie Bernard[2], Azeddine Driouich[2] and Jose M. Seguí-Simarro[1]

[1] COMAV - Universitat Politècnica de València. CPI, Edificio 8E - Escalera I, Camino de Vera, s/n, 46022. Valencia, Spain.

[2] Laboratoire Glycobiologie et Matrice Extracellulaire Végétale (Glyco-MEV)-EA 4358, Plateforme d'Imagerie Cellulaire (PRIMACEN) et Grand Reseau de Recherche VASI de Haute Normandie, Normandie Université, Université de Rouen, 76821 Mont Saint Aignan, Cedex, France

Abstract

In this work, we performed an extensive and detailed analysis of the changes in cell wall composition during *Brassica napus* anther development. We used immunogold labeling to study the spatial and temporal patterns of composition and distribution of different AGP, pectin, xyloglucan and xylan epitopes in high pressure-frozen/freeze-substituted anthers, quantifying and comparing their relative levels in the different anther tissues and developmental stages. We used the following monoclonal antibodies: JIM13, JIM8, JIM14 and JIM16 for AGPs, LM5, LM6, JIM7, JIM5 and LM7 for pectins, CCRC-M1, CCRC-M89 and LM15 for xyloglucan, and LM11 for xylan. Each cell wall epitope showed a characteristic temporal and spatial labeling pattern. Microspore, pollen and tapetal cells showed similar patterns for each epitope, whereas the outermost anther layers (epidermis, endothecium and middle layers) presented remarkably different patterns. Our results suggested that AGPs, pectins, xyloglucan and xylan have specific roles during anther development. The AGP epitopes studied appeared to belong to AGPs specifically involved in microspore differentiation, and contributed first by the tapetum and then, upon tapetal dismantling, by the endothecium and middle layers. In contrast, the changes in pectin and hemicellulose epitopes suggested a specific role in anther dehiscence, facilitating anther wall weakening and rupture. The distribution of the different cell wall constituents is regulated in a tissue and stage-specific manner, which seems directly related with the role of each tissue at each stage.

Keywords: AGPs, cell wall, microspore, pollen, xylan, xyloglucan.

Introduction

Anthers are the plant organs where male gametes are produced and released. Anthers must first develop themselves, then generate the pollen precursors (the pollen mother cells and the microspores), then transform them into pollen grains within which gametes (sperm cells) are produced, and finally open up in a process known as anther dehiscence, to release gamete-containing pollen grains for pollination. All these processes imply changes and adaptations at the tissue and cellular levels to adjust the anthers to these different developmental scenarios. For example, anther dehiscence involves the localized secondary thickening of endothecium walls, coordinated with the degeneration of the anther tapetum and middle layer, the breakdown of the interlocular septa and anther dehydration (reviewed in Wilson et al. 2011). These orchestrated processes of cellular differentiation and degeneration must have a reflection in the cell wall structure and composition. These changes are especially relevant in the case of microspores and pollen grains, which must develop a special coat to provide themselves protection against desiccation and contamination during open air pollen dispersal, but then must be ready to break apart during pollen tube germination.

Apart from cellulose, the main load-bearing component of plant cell walls and present in nearly all cell wall types, other components of the cell wall include arabinogalactan proteins (AGPs), pectins and hemicelluloses. AGPs are a class of ubiquitous proteins characterized by a high degree of glycosylation and the abundant presence of arabinogalactosyl residues (Seifert and Roberts 2007). Glycosylation of AGPs takes place within Golgi stacks through the action of various glycosyltransferase enzymes and then, they are transported via vesicles to the cell wall, where they might undergo additional modifications. AGPs may be attached to the plasma membranes via a glycosylphosphatidylinositol (GPI) lipid anchor, or may be part of the cell walls or of plant secretions (Seifert and Roberts 2007). In cell walls, AGPs have been implicated in different processes related to cell plate formation (Shibaya and Sugawara 2009), the coordination of cell wall assembly (Roy et al. 1998; Vaughn et al. 2007), the maintenance of the solubility of wall polymers prior to being incorporated into the cell wall (Carpita and Gibeaut 1993), or wall plasticity against desiccation (Moore et al. 2013). Aside of their specific role in the cell wall, AGPs have been involved in a myriad of processes related to cell growth, development and reproduction, both *in vivo* and *in vitro.* In plant reproduction, AGPs have been assigned roles in stigma receptivity, pollen-stigma recognition, adhesion and germination, pollen tube growth, guidance through the style and ovary and attraction to the embryo sac, control of the sperm-egg cell fusion, and even in fruit

ripening (reviewed in Pereira et al. 2015). Although there are many reports on the dynamics, distribution and roles of AGPs in female reproductive organs, the amount of data about AGPs in male reproductive organs is comparatively much scarcer (reviewed in Pereira et al. 2015). Besides, most of these data come from *Arabidopsis thaliana*, being very scarce the knowledge available in other species. This is the case, for example, of *Brassica napus*, where the number of studies is rather reduced and limited in scope (El-Tantawy et al. 2013; Southworth and Kwiatkowski 1996). The knowledge of AGP dynamics during anther development in *B. napus* is of special interest because this is a model species for the study of microspore embryogenesis, an experimentally inducible process of outstanding interest for plant breeding, and where AGPs have been shown to have a strong stimulatory effect (Corral-Martínez and Seguí-Simarro 2014; Paire et al. 2003; Tang et al. 2006). The knowledge of the AGP environment of the microspore-containing anthers might provide clues to understand why microspores switch from gametogenesis to embryogenesis.

Pectins are major components present in somatic-type primary cell walls, as well as in other types of specialized walls. For example, the microspore intine was described to have a "pectocellulosic" nature (Sitte 1953). Typically, pectins are synthesized in the Golgi stacks and then transported to the cell wall in a highly methyl esterified form (Zhang and Staehelin 1992). Once in the cell wall, they are de-esterified by pectin methyl esterases, which allow them to cross link via calcium bonds (Drakakaki 2015). In somatic-type cell walls, they are the major structural components of the middle lamella, where they contribute to cell adhesion and tissue cohesion (Bouton et al. 2002; Durand et al. 2009). In particular, homogalacturonan (HG) and rhamnogalacturonan II (RGII) are involved in strengthening the wall (Harholt et al. 2010). However, the role of rhamnogalacturonan I (RGI) is comparatively less known. Pectins have also been implicated in different processes of intercellular signal transduction during plant growth, development and pathogen resistance (reviewed in Malinowski and Filipecki 2002). Such a role implies that the distribution pattern of arabinan- or galactan-containing pectins in plant tissues is regulated during cell growth and development (reviewed in Atmodjo et al. 2013). For example, it is known that arabinans are abundant in the embryo cell walls, but are extensively degraded upon embryo germination in arabidopsis (Gomez et al. 2009). With respect to the study of the distribution and role of the different pectin epitopes during anther development, there are relatively few studies in a limited number of species (Aouali et al. 2001; Costa et al. 2015; Golaszewska and Bednarska 1999; Majewska-Sawka et al. 2004; Peng et al. 2005; Wiśniewska and Majewska-Sawka 2006), and in some cases, they show contradictory results.

The third main group of cell wall polysaccharides is hemicelluloses, where xyloglucan and xylan are two of the most abundant hemicelluloses (Cosgrove 2005). Xyloglucan is the predominant hemicellulose in the primary cell walls of non-graminaceous species (Cosgrove 1997). Xyloglucan is also produced in the Golgi stacks and then exported to the cell wall (reviewed in Drakakaki 2015). They have been proposed to act as cohesive elements to keep cellulose microfibrils together (Marcus et al. 2008), providing structural integrity and strength to the cell wall (Carpita and Gibeaut 1993). Xylans are especially abundant in secondary cell walls and were not thought to be significant components of dicot primary walls (Carpita and Gibeaut 1993), but recent reports point to the notion that the presence of xylans in primary walls has been underreported (Hervé et al. 2009; Mortimer et al. 2015). It was suggested that xyloglucan structure may change as the cell wall matures (Pauly et al. 2001), being also organ and even tissue specific (Freshour et al. 1996; Pauly et al. 2001; Stacey et al. 1995). However, apart from the works of (Majewska-Sawka et al. 2004) in *Beta vulgaris*, to our knowledge there is little information about the different xyloglucan types, and nothing about xylans, present in anther tissues and how they change during anther development. As in the case above mentioned for AGPs, there are studies that associate changes in the xyloglucan and pectic composition of the cell wall with proliferative processes such as the induction of microspore embryogenesis (Barany et al. 2010). However, nothing is known about this in a species like *B. napus*, considered a model for the study of this process.

Hence, in this work we aimed to perform a comprehensive study of the spatial and temporal patterns of composition and distribution of AGPs, pectins and hemicelluloses, including xyloglucan and xylan, during anther development. We used immunogold labeling in conjunction with a set of anti-glycan monclonal antibodies to detect the levels of different AGP, pectin and hemicellulose epitopes in high pressure frozen/freeze substituted tissues of *B. napus* anthers at different stages of microsporogenesis and microgametogenesis. In addition, we quantified and compared the relative levels of the epitopes in the different anther tissues. To our knowledge, this work is the most extensive and detailed study performed to date on the changes in cell wall composition during anther development.

Results

For this work, we selected *B. napus* anthers at three different developmental stages, including 2.4 (Figs. 1A-A''), 3.0 (Fig. 1B-B'') and 3.7 mm-long anthers (Fig. 1C-C''). In 2.4 mm-long anthers, the locule presented principally young-mid microspores (Fig. 1A). In the anther walls (Fig. 1A'), the epidermal layer, the endothecium and the middle layers were clearly visible. The tapetum (Fig. 1A'') was in tight contact with the microspores. 3.0 mm-long anthers were characterized by the presence of vacuolate (mature) microspores (Fig. 1B), defined by an enormous vacuole which occupies most of the volume. At this stage, the epidermis, endothecium and middle layers did not change significantly with respect to the previous stage (Fig. 1B'). The tapetal layer, however, appeared thinner and less organized (Fig. 1B''), as expected for a layer that is disintegrating. 3.7mm-long anthers contained mostly young-mid bicellular pollen grains (Fig. 1C). The thickened endothecium showed the first signs of degradation and the middle layers collapsed, being reduced to a thin strip of degraded material (Fig. 1C'). The tapetum was also dismantled, detached from the anther walls and with the tapetal debris dispersed throughout the locule, surrounding the pollen grains (Fig. 1C''). In the next sections we will present the changes in cell wall composition (based on immunogold labeling of cell wall epitopes) in these five different anther tissues and during the three stages described.

Immunolocalization of AGP epitopes

We used the mAbs JIM8, JIM14, JIM16 and JIM13 to detect and quantify AGPs crossreacting specifically with these antibodies. JIM8 (Supplementary Fig. S1A-C) and JIM14 epitopes (Supplementary Fig. S1D-F) showed a similar distribution pattern, being very scarcely detected in the outer anther layers, including epidermis, endothecium and middle layers, at any of the stages studied. Their levels, however, increased in the cell walls of the tapetal layer of 2.4 and 3.0 mm-long anthers (Fig. 2), which correspond to the stages where the tapetum is not yet fully degraded. They were also found out of the tapetum, in the locular space next to tapetal cells. In microspores, the levels of anti JIM8 and JIM14 labeling in the cytoplasm and the exine were negligible, never different from the background level. However, we observed a higher level of immunogold labeling in the intine and in the locular areas surrounding the exine, in the same stages (2.4 and 3.0 mm-long anthers) where labeling was found in tapetum and the locular space (Supplementary Fig. S1). For JIM16 epitopes, we did not find labeling in any of the anther wall layers studied, with the exception of a very low labeling density (less than 5 particles/μm^2) in the tapetal cell walls, the locule and microspores in 2.4 and 3.0 mm-long anthers (Fig. 2). Together, these data suggest that JIM8, JIM14, and to a much lower extent, JIM16 epitopes would be produced

by the tapetum, would be progressively delivered to the anther locule, and incorporated to the intine. The practical absence of these AGP epitopes in the microspore cytoplasm would indicate that the AGPs found at the intine may come from tapetal delivery. In the intine of pollen grains (from 3.7 mm-long anthers), however, these AGP epitopes were almost or totally absent. Since the tapetum is almost entirely degraded at this stage, it is reasonable to think that these AGP epitopes are no longer released to the locule. However, the levels of these AGP epitopes in the pollen intine, dramatically lower than in the microspore intine, suggest a process of AGP removal and therefore a dynamic regulation of AGPs crossreacting with JIM8, JIM14 and JIM16 in the intine during microspore and pollen development.

With respect to JIM13, immunogold labeling depicted a different scenario, as considerable labeling (40-80 gold particles/μm^2) was observed in all anther tissues and stages studied (Fig. 3). Gold particle decoration was principally found in the cell wall, although some labeling was also observed in the plasma membrane (Fig. 4A). A basal level of AGP epitope detection was also found in the Golgi stacks (Fig. 4A, B), indicating that these AGPs are endogenously produced and then exported to the cell wall. In the epidermis, the levels of JIM13 labeling decreased as the anther developed. Such a decrease, however, was not observed in the endothecium and middle layers. Indeed, the levels of JIM13 labeling dramatically increased in the endothecium of 3.7 mm-long anthers. In the tapetum, the levels of JIM13 labeling found in the Golgi stacks and Golgi-derived secretory vesicles of 2.4 (Fig. 4C) and 3.0 mm-long anthers (but not 3.7 mm-long) were dramatically higher than in the other anther layers (Fig. 3). Consistent with this, the levels of these AGP epitopes found in the tapetal cell walls, in the anther locule, and in the microspore intine (Fig. 4E) were the highest, up to 170 gold particles/μm^2 (Fig. 3). In the cytoplasm of developing microspores, labeling was also significantly higher than background, which suggested that in addition to the high contribution of the tapetum, these AGPs were being actively synthesized by the microspores as well. In the 3.7 mm-long stage, pollen cells presented no JIM13 labeling in the Golgi stacks and vesicles. In the tapetum, labeling was lower than in previous stages, being dispersed through the tapetal remnants (Fig. 4D). Consistently, the levels found in the pollen intine (Fig. 4F) were also lower and similar to those of the wall of the generative cell (Fig. 4G), being most of the labeling at this stage concentrated in the anther locule (Fig. 3). Together, these results indicate that the levels of JIM13-crossreacting AGPs in the different anther tissues change during development, but in a manner different than that for JIM8, JIM14 and JIM16-recognized epitopes.

Immunolocalization of pectin epitopes

We used LM5, LM6, LM7, JIM5 and JIM7 antibodies to detect and quantify pectin epitopes (see Table 1). Quantitative results are shown in Fig. 5. For LM5 (Supplementary Fig. S2A, B), LM6 (Fig. 6A, C), JIM7 (Supplementary Fig. S2C, D) and LM7 antibodies (Supplementary Fig. S2E, F), immunogold labeling was similar in the middle lamella and the rest of the cell wall. Thus, all the cell wall labeling was considered in a single category for these antibodies. Only JIM5 labeling results were different between the middle lamella and the rest of the cell wall (Fig. 6B). This is why in this case labeling density is shown in two separated categories in Fig. 5. In general, the results obtained evidenced that the level of pectins and the proportion of the different pectic epitopes in the cell walls of anther cells is different for each tissue layer and for each developmental stage. In particular, LM5-crossreacting epitopes ((1-4)-β-D-galactans) were especially abundant in the epidermis (Supplementary Fig. S2A), and their levels increased as the anther progressed in development. In inner layers, levels were progressively lower. In contrast, a different situation was observed for LM6-crossreacting epitopes ((1-5)-α-L-arabinans), which were abundant in the epidermis, middle layers and principally in the endothecium (Fig. 6A), but their levels decreased as the anther progressed in development. LM6 has no cross-reactivity with gum Arabic, although according to manufacturer specifications, it may recognize AGPs in some species, in addition to (1-5)-α-L-arabinans. However, considering the quantification patterns of the four anti-AGP antibodies used, and their striking differences with the pattern of LM6 observed, we can assume that at least in *B. napus*, LM6 would not be recognizing any of the AGPs recognized by the anti-AGP antibodies used hereby.

JIM7-crossreacting epitopes (highly methyl-esterified homogalacturonans) were found in approximately similar levels in epidermis (Supplementary Fig. S2C), endothecium and middle layers, and increased during anther development. In parallel, JIM5-crossreacting epitopes (low methyl-esterified homogalacturonans) were principally found in 2.4 mm-long anthers, in approximately similar low levels in epidermis, endothecium and middle layers. This epitope showed a specific abundance in the middle lamella of these walls in endothecium (Fig. 6B) and middle layers. Consistent with the progressively higher levels of highly methyl-esterified pectins and the progressively lower levels of low methyl-esterified pectins, LM7 immunolocalization showed that the levels of partially methyl-esterified homogalacturonans resulting from non-blockwise de-esterification were progressively lower as the anther proceeds through microsporogenesis and microgametogenesis (compare Supplementary Fig. S2E and F). These results suggested that pectin de-esterification would occur in the first stages of anther development, being progressively inhibited in maturing anthers.

The pectic composition and distribution observed for the epidermis, endothecium and middle layers contrasted dramatically with that found for the tapetum and the microspores. Consistent with tapetal degradation, no noticeable (different from background) signal was found for any of the pectin epitopes studied in the tapetum at any stage. In microspores, the general levels were very low in the intine and the surrounding locular space, decreasing as the microspore transforms into a pollen grain (Fig. 5; Supplementary Fig. S2B, D). The highest levels of pectin immunolocalization were observed for the (1-5)-α-L-arabinans detected with LM6, which accumulated in similar amounts in the intine of microspores (Fig. 6C) and maturing pollen grains. Interestingly, low esterified (Fig. 6D) and highly methyl-esterified homogalacturonans (Supplementary Fig. S2D) were very scarcely found in the intine, but were more abundant in the locular region surrounding the microspores and pollen grains. In particular, low-esterified homogalacturonans detected with JIM5 were specifically found in the material deposited at the exine surface (asterisk in Fig. 6D).

Immunolocalization of hemicelluloses

We used CCRC-M1, CCRC-M89 and LM15 antibodies to detect and quantify xyloglucan epitopes, and LM11 to detect and quantify xylan epitopes (see Table 1). Quantitative results are shown in Fig. 7. In general, immunogold labeling with all the anti-xyloglucan antibodies concentrated in the cell walls of the epidermal cells (Supplementary Fig. S3A, C), endothecium (Fig. 8A, B) and middle layers. Within the walls, we could not find a preferred localization of these epitopes in the middle lamella. Among the three anti-xyloglucan antibodies, the highest labeling density was obtained with CCRC-M1 (Fig. 8A, B), indicating that fucosylated xyloglucan is the most abundant in these tissues. In general, the highest labeling density was observed in the first stages (2.4 and 3.0 mm-long anthers), and with the exception of CCRC-M89, the lowest was observed in all the tissues of 3.7 mm-long anthers, being null in some cases (Fig. 7). As also observed for pectins, labeling with the three anti-xyloglucan antibodies in the tapetal cell walls, when present, was very low. In microspores/pollen, intine labeling was also very scarce (Supplementary Fig. S3B, D). Xylan epitopes were detected in the anther walls with higher labeling densities in the first stages and outer anther layers (Fig. 8C). The microspore and pollen intine was also decorated, and a low but noticeable signal was observed in the material deposited at the exine surface (Fig. 8D).

Discussion

AGPs could be involved in pollen differentiation

All of the antibodies we used have been previously employed to identify the corresponding epitopes in different species, plant organs and tissues, including anthers at different developmental stages (Coimbra et al. 2007; Costa et al. 2015; Wiśniewska and Majewska-Sawka 2006). In general, results have been remarkably diverse among species. For example, in Arabidopsis and *Quercus suber*, no differences were found between JIM13 and JIM8 localization and signal levels (Coimbra et al. 2007; Costa et al. 2015), while in *B. napus* we found JIM8 levels remarkably lower than JIM13, but with a pattern similar to that of Arabidopsis and *Quercus*, restricted to the tapetum and the microspores/pollen. The fact that different species show similar temporal and spatial expression patterns for different AGP epitopes may suggest that at least one glycoprotein with a similar role in different species, could be glycosylated in a different manner for each species. Another common pattern was the abundance of the recognized epitopes in the inner parts of the anther. Indeed, all the antibodies but JIM13 showed almost no labeling in the outer layers. For JIM13, although there was labeling in all anther tissues and stages, the levels in the tapetum, locular fluid and microspores/pollen were dramatically higher. It is reasonable to think that such an abundant and permanent presence of JIM13 epitopes in the anther locule must imply an important role for these AGPs. Thus, the question then arises as to what this role is? AGPs might be involved in the accumulation of calcium needed for different reproductive events. It is known that both AGPS and calcium signaling are needed for pollen tube growth and then for gamete fusion during fertilization (Antoine et al. 2000; Coimbra et al. 2007). Recently, it was proposed that cell wall AGPs might act as calcium capacitors to release calcium to the cell when needed (Lamport and Varnai 2013). According to the AGP expression patterns we showed, it seems unlikely that these AGPs are being accumulated to assist in calcium signaling during pollen tube growth, because their levels in the intine of maturing pollen dramatically dropped down in all cases. Alternatively, based on the presence of JIM13 epitopes in the generative and sperm cells of angiosperms such as *B. napus*, *B. campestris* and *Lilium longiflorum* pollen, and also in male and female fern gametes a role for AGPs in pollen maturation and gamete function was proposed (El-Tantawy et al. 2013; Lopez and Renzaglia 2014, 2016; Southworth and Kwiatkowski 1996). With a wider perspective, the fact that all four AGP epitopes studied show higher levels in the microspores/pollen, the tapetum, and the anther locule, suggest that, as proposed by Coimbra et al. (2007), AGPs might possibly act as cell differentiation signals, either directly or indirectly

through calcium accumulation. In such a case, their involvement would be in the differentiation of microspores, where their levels are high, towards mature pollen, where their levels decrease.

The endothecium and middle layers are also an important source of some AGPs and pectins for microspore/pollen development

In general, the labeling patterns of the four AGP epitopes studied were similar in terms of showing the highest labeling density in 3.0 mm-long anthers and being lower in mature anthers. An exception to this was the endothecium and middle layers, where JIM13 antibodies showed a remarkably high labeling density in mature anthers. According to our results, JIM13 epitopes seem to be actively synthesized during the first stages and delivered to the anther locule. The presence of JIM13 epitopes found in the Golgi stacks and vesicles of microspores suggests that its occurrence in the microspore coat would have two parallel origins: the microspore itself and the delivery from the anther wall to the locule. This pattern, however, changed after pollen mitosis I, where JIM13 signal occurred in the cell wall of the generative cell, their levels decreased in the pollen intine, stayed high in the locule, and reached their highest values in the endothecium and middle layers. This suggests that JIM13 epitope levels must be kept high in the *B. napus* anther locule during all anther developmental stages, and it seems that nearly all anther tissues would be implicated, in a sequential manner, in the delivery of JIM13 epitopes to keep the locular levels high. First, these AGPs would be contributed by the tapetum and microspores, and upon tapetum disintegration, they would be contributed mostly by the endothecium and middle layers. The scenario for JIM8 and JIM14 would be somehow different. Our results indicated that they might be produced and delivered to the locule by the tapetum. However, upon tapetum dismantling in 3.7 mm-long anthers, these epitopes are not detected in any other anther layer and their locular levels drop down dramatically. Therefore, these AGPs would be specifically needed during the first stages of anther development, i.e. microsporogenesis rather than microgametogenesis.

As proposed by Aouali et al. (2001) the low levels of pectins in the microspore/pollen cytoplasm and the higher levels found in the locular fluid account for a locular origin for, at least, part of the pectins of the microspore/pollen wall. Indeed, pectins have traditionally been reported to come from the degradation of tapetal and/or meiocyte walls (Owen and Makaroff 1995), or from tapetum metabolism and secretion (Aouali et al. 2001). We did not detect pectin epitopes in the tapetum. Similar studies in other species found JIM5, LM5 and LM6 epitopes in the tapetum of *Quercus suber* (Costa et al. 2015), but not of *Beta vulgaris* (Majewska-Sawka et

al. 2004), *Lolium perenne* (Wiśniewska and Majewska-Sawka 2006) and *Cucumis sativus* (Peng et al. 2005). JIM7 epitopes have been found in the tapetum of *Quercus suber* (Costa et al. 2015), *Beta vulgaris* (Majewska-Sawka et al. 2004), *Lilium* (Aouali et al. 2001) and *Lolium perenne* (Wiśniewska and Majewska-Sawka 2006). In light of all these data, it seems that the expression of these epitopes in the tapetum cell wall is species-specific. However, these epitopes were found in the locular fluid and in the microspore and/or pollen coat of the above mentioned species, and also pepper (Barany et al. 2010) and *B. napus* (our results). Since in *B. napus* this contribution cannot be exclusively attributed neither to the tapetum nor to the microspores/pollen, we may assume that pectin release would come from the degradation of the middle lamellae and/or the endothecium, where we observed the highest levels. Therefore, it appears that the endothecium and middle layers have also a prominent role in the contribution of pectins and AGPs (at least those crossreacting with JIM13) to the anther locule and the microspore/pollen intine.

Specific changes in pectin composition would prepare anthers for dehiscence

We showed that the pectin composition of anther walls changes dramatically during development. Indeed, pectins of the epidermis cell walls are rich in galactan epitopes crossreacting with LM5, and their levels increase during anther development. However, these pectins are less represented in the endothecium and middle layers. In contrast, the levels of arabinan epitopes crossreacting with LM6 are higher in the endothecium and middle layers than in the epidermis, but their levels decrease during anther development in the three layers. There seems to be a replacement of arabinans by galactans, at least in the epidermis, possibly due to the *de novo* synthesis of pectins and/or to their *in situ* remodeling. In general, abundance of LM6-recognized epitopes is associated to rapidly growing cells, whereas abundance of LM5-recognized epitopes seems to be associated to maturing tissues (Vaughn 2003). Previous studies have related the increase of galactose side-chains in pectins of differentiating and elongating cells with the increase in cell wall firmness (Majewska-Sawka et al. 2004; McCartney et al. 2000; McCartney et al. 2003; Willats et al. 1999). In parallel, actively proliferating cells present an opposite scenario, with very low amounts of galactose residues, and abundance of arabinose residues (Kikuchi et al. 1995; Majewska-Sawka and Münster 2003; Majewska-Sawka et al. 2004; Willats et al. 1999). Therefore, the replacement of arabinans by galactans in epidermal cells would be indicating a transition to differentiation of these cells, prior to dehiscence. In several Southern African resurrection plants, enrichment in arabinan-containing carbohydrates provides cell walls with plasticity and flexibility, allowing them to withstand

long periods of dessication (Moore et al. 2013). According to this, the replacement of arabinans by galactans would make these walls less flexible and resistant to dessication, thus facilitating anther dehiscence for pollen dispersal.

The most dramatic changes were observed for JIM7, JIM5 and LM7 epitopes. Willats et al. (2001) demonstrated that the pattern and degree of pectin methylation have a direct impact on the mechanical and physiological properties of calcium-mediated pectin gels, which may modulate the functionalities of pectic homogalacturonan domains. In particular, they showed that pectins enriched in LM7 recognized-epitope have a prominent role in maintaining cell wall adhesion, possibly through the establishment of an appropriate environment for processes that directly maintain cell adhesion. Our LM7 labeling results showed that this epitope is abundant during the early stages of anther development, being progressively lost, and absent in anthers close to dehiscence. This was paralleled by a progressive increase of the levels of highly methyl-esterified pectins detected with JIM7, and a decrease of the levels of low esterified pectins detected with JIM5. Thus, it is tempting to speculate that in the enzymatic breakdown of the cell walls occurring as the anther prepares for dehiscence, the LM7 epitope would be progressively removed, facilitating the action of pectin-degrading enzymes and the loosening of the anther cell wall. Although similar, this dynamics may be slightly different between species, as shown in *Allium cepa* (Golaszewska and Bednarska 1999). In summary, our results together with the studies above cited suggest that in general, pectins may have a specialized role in reproductive tissues, substantially different from the structural role usually assigned to them in somatic cell walls (Carpita and Gibeaut 1993). In the particular case of *B. napus* anthers, these roles could be related to dehiscence.

Hemicelluloses seem not related with pollen development but with anther maturation

As with the anti-pectin and anti-AGP antibodies, the three anti-xyloglucan antibodies showed different levels of immunogold labeling. However, the temporal and spatial patterns of xyloglucan detection were similar, being principally detected in the first two stages and concentrated in the outermost anther tissues, as in *Beta vulgaris* with the CCRC-M1 antibody (Majewska-Sawka et al. 2004). The absence of xyloglucan in the cell walls of anther tissues more directly related with pollen development and gametogenesis suggest that xyloglucan would not be related with these processes. Instead, they seem to have a more specific role in the anther wall tissues. In the particular case of fucosylated xyloglucan (recognized by CCRC-M1) it is known that fucose residues are important for the establishment of xyloglucan-cellulose interactions to provide tensile strength (Peña et al. 2004).

Thus, a reduction in fucosylated residues during anther maturation could be a mechanism to facilitate anther wall weakening and further rupture. Working with stem segment cells of *Pisum sativum*, Pauly et al. (2001) proposed a relationship between the xyloglucan type and the status of cell wall maturation, establishing a correlation between cell elongation and the conversion of XXXG to XXG. Our results with the LM15 antibody recognizing XXXG xyloglucan motifs showed a decrease as the anther elongates during maturation. In contrast, the CCRC-M89 antibody, recognizing xyloglucan motifs with no XXXG showed a clear increase. Our results would be consistent with the proposal of Pauly et al. (2001), confirming that an increase in xyloglucan without XXXG motifs is a typical feature of elongating cell walls of maturing anthers. Xylan detected with the LM11 antibody exhibited a labeling pattern similar to those of CCRC-M1 and LM15 anti-xyloglucan antibodies, which suggests that xylan would have a role similar to these xyloglucan in anther dehiscence. Indirect support to this notion comes from the fact that the Arabidopsis *irx8* mutant, deficient in lignin and xylan biosynthesis, produces indehiscent anthers (Hao et al. 2014). Besides, this study adds to the increasing body of data pointing out that xylan is also present in the primary wall of some species and cell types (Hervé et al. 2009; Mortimer et al. 2015).

Concluding remarks

Considering all the results together, we can deduce that the microspores/pollen and the tissue directly involved in their development, the tapetum, showed remarkably similar labeling patterns for each epitope, whereas the three outermost anther wall layers (epidermis, endothecium and middle layers) markedly differed from these patterns. This indicates that the cell wall metabolism of these adjacent cells is regulated in a totally different manner, consistent with the different roles of each tissue type. We can also deduce that all the carbohydrates and glycoproteins studied have specific roles during *B. napus* anther development. However, one can find a remarkable difference between the distribution patterns of the studied AGPs on one hand, and pectins and hemicelluloses on the other hand. In the first case, we found evidences that suggest that the epitopes studied belong to AGPs acting as cell differentiation signals, specifically involved in microspore differentiation. These AGPs would be mainly contributed first by the tapetum, and later on by the endothecium and middle layers, after tapetal disintegration. In contrast, the changes in pectin and hemicellulose composition suggested that aside their known structural roles, they would have a specialized role related to anther dehiscence, facilitating wall weakening and rupture. In summary, we have shown that the different cell wall components are regulated in a

different manner in different anther tissues and developmental stages, and this regulation is directly related with the role of each tissue at each stage.

Materials and methods

Plant material

B. napus L. cv. Topas (line DH4079) plants were grown in the greenhouses of the COMAV Institute (Universitat Politècnica de València, Valencia, Spain) during spring months under controlled temperature (~20ºC) and natural light.

Processing of B. napus anthers for transmission electron microscopy

Anthers carrying microspores and pollen grains at different stages of microsporogenesis and microgametogenesis were processed basically as described in Seguí-Simarro (2015). In brief, anthers were excised, transferred to aluminum sample holders, cryoprotected with 150 mM sucrose, frozen in a Leica EM HPM-100 high-pressure freezer (Leica Microsystems, Vienna), and then transferred to LN_2. Samples were freeze substituted in a Leica AFS2 system (Leica Microsystems, Vienna) with 2% OsO_4 in anhydrous acetone at -80ºC for 7 days, followed by slow warming to room temperature over a period of 2 days. After rinsing in several acetone washes, they were removed from the holders, rinsed again in acetone, and infiltrated with increasing concentrations of Epon resin (Ted Pella, Redding, CA) in acetone according to the following schedule: 4 h in 5% resin, 4 h in 10% resin, 12 h in 25% resin, and 24 h in 50, 75, and 100% resin, respectively. Polymerization was performed at 60ºC for 2 days. At least five resin blocks containing one anther were obtained for each anther stage. Using a Leica UC6 ultramicrotome, thin sections (1 μm) were obtained for light microscopy observation, and ~80 nm sections were obtained for electron microscopy of at least three different bocks of each stage. Sections were mounted on formvar-coated, 200 mesh copper grids, stained with uranyl acetate and lead citrate, and observed in a Jeol JEM 1010 electron microscope.

Immunogold labelling

For the detection of AGPs we used the following primary antibodies: JIM13, a rat IgM monoclonal antibody (mAb) recognizing the AGP2 epitope present in different plant exudates such as gum Arabic and gum ghatti (Knox et al. 1991); JIM8, a mAb (rat IgG2c) recognizing an AGP expressed during reproductive development in

B. napus (Pennell et al. 1991); JIM14, a mAb (rat IgM) recognizing an unknown AGP epitope different from that recognized by JIM13 (Knox et al. 1991); JIM16, a mAb (rat IgM) recognizing an unknown AGP present in different plant exudates such as gum arabic, gum ghatti and gum karaya (Knox et al. 1991). For the detection of pectins we used the following antibodies: LM5, a mAb (rat IgG) crossreacting with (1-4)-β-D-galactosyl residues associated with the pectic polymer rhamnogalacturonan-I (Jones et al. 1997); LM6, a mAb (rat IgG) crossreacting with (1-5)-α-L-arabinans (Willats et al. 1998); JIM7, a mAb (rat IgA) crossreacting with highly methyl-esterified epitopes of the homogalacturonan domain of pectic polysaccharides (Knox et al. 1990; Willats et al. 2000); JIM5, a mAb (rat IgG) crossreacting with low methyl-esterified epitopes of homogalacturonan (Knox et al. 1990; Willats et al. 2000); LM7, a mAb (rat IgM) crossreacting with partially methyl-esterified pectin homogalacturonan that results from non-blockwise de-esterification processes (Willats et al. 2001). For the detection of xyloglucan we used the following antibodies: CCRC-M1, a mAb (mouse IgG1) specific for fucosyalated xyloglucan (Pattathil et al. 2010); CCRC-M89, a mAb (mouse IgG1) which binds to non-XXXG xyloglucan oligosaccharides (Pattathil et al. 2010); LM15, a mAb (rat IgG2c) crossreacting with the XXXG motif of xyloglucan (Marcus et al. 2008). For xylan detection we used LM11, a mAb (rat IgM) which recognizes arabinoxylan and low-substituted xylans (McCartney et al. 2005). For more information about the antibodies, see Table 1.

Immunogold labeling was performed in HPF-fixed, OsO_4-treated, epoxy-embedded samples. This processing is not compatible with immunolocalization of protein epitopes, because OsO_4 is likely to alter protein epitopes. However, this procedure can be successfully used to specifically detect carbohydrate epitopes (Otegui et al. 2002; Otegui and Staehelin 2004; Parra-Vega et al. 2015), not so sensitive to OsO_4. Thus, by using this approach, we were able to combine specific immunolabeling with excellent ultrastructural preservation. For immunolocalization of cell wall components, we deposited Epon sections (80-100 nm) onto Formvar and carbon-coated, 200-mesh nickel grids (Electron Microscopy Sciences). Sections were hydrated with 1x Tris buffered saline (TBS) + 0.2% BSA for 3 min, blocked with TBS + 0.2% BSA + 3% skimmed milk for 30 min. After a quick wash in TBS + 0.2% BSA, sections were incubated with the corresponding primary antibody, according to Table 1, diluted in TBS + 0.2% BSA for 3h at 25ºC. Next, sections were washed with TBS + 0.2% BSA six times, 5 min each, and incubated with the corresponding secondary antibodies (see Table 1) conjugated with 10 nm colloidal gold (all from BBI Solutions, UK), diluted 1:25 in TBS + 0.2% BSA, for 1 hour at 25ºC. After five 5-min washes with TBS + 0.2% BSA and a 1-min wash with TBS, sections were postfixed with 2%

glutaraldehyde in TBS for 10 min, washed (5 min) once in TBS and twice in distilled water. Sections were counterstained with 0.5% uranyl acetate in 70% methanol (6 min) and lead citrate (30 s). Controls were performed excluding primary antibodies and keeping unchanged the rest of the protocol.

Quantification of immunogold labeling

In order to exclude as many variables as possible for quantification, we processed at the same time anther samples of different developmental stages. Once embedded and sectioned, immunogold labelings were also performed at the same time for all AGPs, all pectins and all xyloglucan and xylan. Sampling was carried out over a number of micrographs taken randomly from all the cells of interest on each grid of each of the resin blocks used for each anther stage. The minimum number of micrographs to take was determined using the progressive mean test (Williams 1977), with a minimum confidence limit of α=0.05. In general, this test provided minimum numbers between 15-20 micrographs per antibody, stage and tissue studied. Labeling density was defined as the number of particles per area unit (μm^2). This number of particles was determined by hand counting particles over the compartments under study. These compartments were (1) the cytoplasmic Golgi stacks and vesicles, (2) the cell wall, differentiating between middle lamella and the rest of the cell wall when differences between both regions were detected, (3) the intine for microspores and pollen, and (4) the locular space separating the microspores/pollen from the innermost anther wall layer. As an estimation of background noise, we determined the particle density over regions where the presence of the studied carbohydrates is not expected. These regions included the cytoplasm (excluding the Golgi stacks and Golgi-derived vesicles), cytoplasmic organelles and nucleus. Background noise never exceeded 5%, compared to the quantified signal. The area in μm^2 was measured using a square lattice composed of 11 x 16 squares of 15 x 15 mm each. For each stage and tissue, labeling density was expressed as the mean labeling density of all micrographs ± SD. Comparisons between mean labeling densities among stages and among tissue and subcellular regions were performed by one-way ANOVA tests using Statgraphics software. Means were separated using a Tukey's test with $p \leq 0.05$. Labeling densities and statistical comparisons were shown as independent histograms for each antibody and tissue. In order to facilitate comparisons between tissues, all the histograms were built using the same Y-axis scale, although in some cases, this led to the occurrence of empty or almost empty charts.

Funding

This work was supported by the Spanish Ministry of Economy (MINECO) jointly funded by FEDER [Grants AGL2010-17895, AGL2014-55177 to JMSS]. A.D is grateful to La Région de Haute Normandie and le Grand Réseau de Recherche-Végétal, Agronomie, Sol et Innovation, l'Université de Rouen, Le Fonds Européen FEDER, and l'ANR for financial support.

Conflicts of interest

No conflicts of interest declared.

Acknowledgements

We want to express our thanks for their excellent technical help to the staff of the Electron Microscopy Service of Universitat Politècnica de València.

References

Antoine, A.F., Faure, J.-E., Cordeiro, S., Dumas, C., Rougier, M. and Feijó, J.A. (2000) A calcium influx is triggered and propagates in the zygote as a wavefront during in vitro fertilization of flowering plants. *Proceedings of the National Academy of Sciences* 97: 10643-10648.

Aouali, N., Laporte, P. and Clement, C. (2001) Pectin secretion and distribution in the anther during pollen development in *Lilium*. *Planta* 213: 71-79.

Atmodjo, M.A., Hao, Z.Y. and Mohnen, D. (2013) Evolving Views of Pectin Biosynthesis. In *Annual Review of Plant Biology, Vol 64*. Edited by Merchant, S.S. pp. 747-+. Annual Reviews, Palo Alto.

Barany, I., Fadon, B., Risueno, M.C. and Testillano, P.S. (2010) Cell wall components and pectin esterification levels as markers of proliferation and differentiation events during pollen development and pollen embryogenesis in *Capsicum annuum* L. *J. Exp. Bot.* 61: 1159-1175.

Bouton, S., Leboeuf, E., Mouille, G., Leydecker, M.-T., Talbotec, J., Granier, F., et al. (2002) *QUASIMODO1* Encodes a Putative Membrane-Bound Glycosyltransferase Required for Normal Pectin Synthesis and Cell Adhesion in Arabidopsis. *The Plant Cell* 14: 2577-2590.

Carpita, N.C. and Gibeaut, D.M. (1993) Structural models of primary cell walls in flowering plants: consistency of molecular structure with the physical properties of the walls during growth. *The Plant Journal* 3: 1-30.

Coimbra, S., Almeida, J., Junqueira, V., Costa, M.L. and Pereira, L.G. (2007) Arabinogalactan proteins as molecular markers in Arabidopsis thaliana sexual reproduction. *J. Exp. Bot.* 58: 4027-4035.

Corral-Martínez, P. and Seguí-Simarro, J.M. (2014) Refining the method for eggplant microspore culture: effect of abscisic acid, epibrassinolide, polyethylene glycol, naphthaleneacetic acid, 6-benzylaminopurine and arabinogalactan proteins. *Euphytica* 195: 369-382.

Cosgrove, D.J. (1997) Assembly and enlargement of the primary cell wall in plants. *Annual Review of Cell and Developmental Biology* 13: 171-201.

Cosgrove, D.J. (2005) Growth of the plant cell wall. *Nat Rev Mol Cell Biol* 6: 850-861.

Costa, M.L., Sobral, R., Ribeiro Costa, M.M., Amorim, M.I. and Coimbra, S. (2015) Evaluation of the presence of arabinogalactan proteins and pectins during Quercus suber male gametogenesis. *Ann. Bot.* 115: 81-92.

Drakakaki, G. (2015) Polysaccharide deposition during cytokinesis: Challenges and future perspectives. *Plant Sci.* 236: 177-184.

Durand, C., Vicré-Gibouin, M., Follet-Gueye, M.L., Duponchel, L., Moreau, M., Lerouge, P., et al. (2009) The Organization Pattern of Root Border-Like Cells of Arabidopsis Is Dependent on Cell Wall Homogalacturonan. *Plant Physiol.* 150: 1411-1421.
El-Tantawy, A.-A., Solís, M.-T., Costa, M.L., Coimbra, S., Risueño, M.-C. and Testillano, P.S. (2013) Arabinogalactan protein profiles and distribution patterns during microspore embryogenesis and pollen development in *Brassica napus*. *Plant Reprod* 26: 231-243.
Freshour, G., Clay, R.P., Fuller, M.S., Albersheim, P., Darvill, A.G. and Hahn, M.G. (1996) Developmental and Tissue-Specific Structural Alterations of the Cell-Wall Polysaccharides of *Arabidopsis thaliana* Roots. *Plant Physiol.* 110: 1413-1429.
Golaszewska, B. and Bednarska, E. (1999) Immunocytochemical localization of pectins in the maturing anther of *Allium cepa* L. *Folia Histochem. Cytobiol.* 37: 199-208.
Gomez, L.D., Steele-King, C.G., Jones, L., Foster, J.M., Vuttipongchaikij, S. and McQueen-Mason, S.J. (2009) Arabinan metabolism during seed development and germination in Arabidopsis. *Mol. Plant.* 2: 966-976.
Hao, Z.Y., Avci, U., Tan, L., Zhu, X., Glushka, J., Pattathil, S., et al. (2014) Loss of Arabidopsis GAUT12/IRX8 causes anther indehiscence and leads to reduced G lignin associated with altered matrix polysaccharide deposition. *Frontiers in Plant Science* 5.
Harholt, J., Suttangkakul, A. and Vibe Scheller, H. (2010) Biosynthesis of Pectin. *Plant Physiol.* 153: 384-395.
Hervé, C., Rogowski, A., Gilbert, H.J. and Knox, J.P. (2009) Enzymatic treatments reveal differential capacities for xylan recognition and degradation in primary and secondary plant cell walls. *The Plant Journal* 58: 413-422.
Jones, L., Seymour, G.B. and Knox, J.P. (1997) Localization of pectic galactan in tomato cell walls using a monoclonal antibody specific to (1[->]4)-[beta]-D-galactan. *Plant Physiol.* 113: 1405-1412.
Kikuchi, A., Satoh, S., Nakamura, N. and Fujii, T. (1995) Differences in pectic polysaccharides between carrot embryogenic and non-embryogenic calli. *Plant Cell Rep.* 14: 279-284.
Knox, J.P., Linstead, P.J., King, J., Cooper, C. and Roberts, K. (1990) Pectin esterification is spatially regulated both within cell walls and between developing tissues of root apices. *Planta* 181: 512-521.
Knox, J.P., Linstead, P.J., Peart, J., Cooper, C. and Roberts, K. (1991) Developmentally regulated epitopes of cell surface arabinogalactan proteins and their relation to root tissue pattern formation. *Plant J.* 1: 317-326.
Lamport, D.T. and Varnai, P. (2013) Periplasmic arabinogalactan glycoproteins act as a calcium capacitor that regulates plant growth and development. *New Phytologist* 197: 58-64.
Lopez, R.A. and Renzaglia, K.S. (2014) Multiflagellated sperm cells of *Ceratopteris richardii* are bathed in arabinogalactan proteins throughout development. *Am. J. Bot.*
Lopez, R.A. and Renzaglia, K.S. (2016) Arabinogalactan proteins and arabinan pectins abound in the specialized matrices surrounding female gametes of the fern Ceratopteris richardii. *Planta* 243: 947-957.
Majewska-Sawka, A. and Münster, A. (2003) Cell-wall antigens in mesophyll cells and mesophyll-derived protoplasts of sugar beet: possible implication in protoplast recalcitrance? *Plant Cell Rep.* 21: 946-954.
Majewska-Sawka, A., Munster, A. and Wisniewska, E. (2004) Temporal and spatial distribution of pectin epitopes in differentiating anthers and microspores of fertile and sterile sugar beet. *Plant Cell Physiol.* 45: 560-572.
Malinowski, R. and Filipecki, M. (2002) The role of cell wall in plant embryogenesis. *Cell. Mol. Biol. Lett.* 7: 1137-1151.
Marcus, S., Verhertbruggen, Y., Herve, C., Ordaz-Ortiz, J., Farkas, V., Pedersen, H., et al. (2008) Pectic homogalacturonan masks abundant sets of xyloglucan epitopes in plant cell walls. *BMC Plant Biol.* 8: 60.
McCartney, L., Marcus, S.E. and Knox, J.P. (2005) Monoclonal Antibodies to Plant Cell Wall Xylans and Arabinoxylans. *Journal of Histochemistry & Cytochemistry* 53: 543-546.
McCartney, L., Ormerod, A.P., Gidley, M.J. and Knox, J.P. (2000) Temporal and spatial regulation of pectic (1→4)-β-D-galactan in cell walls of developing pea cotyledons: implications for mechanical properties. *The Plant Journal* 22: 105-113.

McCartney, L., Steele-King, C.G., Jordan, E. and Knox, J.P. (2003) Cell wall pectic (1→4)-β-d-galactan marks the acceleration of cell elongation in the Arabidopsis seedling root meristem. *The Plant Journal* 33: 447-454.
Moore, J.P., Nguema-Ona, E.E., Vicre-Gibouin, M., Sorensen, I., Willats, W.G., Driouich, A., et al. (2013) Arabinose-rich polymers as an evolutionary strategy to plasticize resurrection plant cell walls against desiccation. *Planta* 237: 739-754.
Mortimer, J.C., Faria-Blanc, N., Yu, X.L., Tryfona, T., Sorieul, M., Ng, Y.Z., et al. (2015) An unusual xylan in Arabidopsis primary cell walls is synthesised by GUX3, IRX9L, IRX10L and IRX14. *Plant J.* 83: 413-527.
Otegui, M.S., Capp, R. and Staehelin, L.A. (2002) Developing seeds of Arabidopsis store different minerals in two types of vacuoles and in the endoplasmic reticulum. *Plant Cell* 14: 1311-1327.
Otegui, M.S. and Staehelin, L.A. (2004) Electron tomographic analysis of post-meiotic cytokinesis during pollen development in *Arabidopsis thaliana*. *Planta* 218: 501-515.
Owen, H. and Makaroff, C.A. (1995) Ultrastructure of microsporogenesis and microgametogenesis in *Arabidopsis thaliana* (L.) Heynh. ecotype Wassilewskija (Brassicaceae). *Protoplasma* 185: 7-21.
Paire, A., Devaux, P., Lafitte, C., Dumas, C. and Matthys-Rochon, E. (2003) Proteins produced by barley microspores and their derived androgenic structures promote in vitro zygotic maize embryo formation. *Plant Cell Tissue Organ Cult.* 73: 167-176.
Parra-Vega, V., Corral-Martínez, P., Rivas-Sendra, A. and Seguí-Simarro, J.M. (2015) Induction of embryogenesis in *Brassica napus* microspores produces a callosic subintinal layer and abnormal cell walls with altered levels of callose and cellulose. *Frontiers in Plant Science* 6: 1018.
Pattathil, S., Avci, U., Baldwin, D., Swennes, A.G., McGill, J.A., Popper, Z., et al. (2010) A comprehensive toolkit of plant cell wall glycan-directed monoclonal antibodies. *Plant Physiol.* 153: 514-525.
Pauly, M., Qin, Q., Greene, H., Albersheim, P., Darvill, A. and York, W.S. (2001) Changes in the structure of xyloglucan during cell elongation. *Planta* 212: 842-850.
Peng, Y.B., Zou, C., Gong, H.Q., Bai, S.N., Xu, Z.H. and Li, Y.Q. (2005) Immunolocalization of arabinogalactan proteins and pectins in floral buds of cucumber (Cucumis sativus L.) during sex determination. *J. Integr. Plant Biol.* 47: 194-200.
Pennell, R.I., Janniche, L., Kjellbom, P., Scofield, G.N., Peart, J.M. and Roberts, K. (1991) Developmental Regulation of a Plasma Membrane Arabinogalactan Protein Epitope in Oilseed Rape Flowers. *The Plant Cell* 3: 1317-1326.
Peña, M.J., Ryden, P., Madson, M., Smith, A.C. and Carpita, N.C. (2004) The galactose residues of xyloglucan are essential to maintain mechanical strength of the primary cell walls in Arabidopsis during growth. *Plant Physiol.* 134: 443-451.
Pereira, A.M., Pereira, L.G. and Coimbra, S. (2015) Arabinogalactan proteins: rising attention from plant biologists. *Plant Reprod* 28: 1-15.
Roy, S., Jauh, G.Y., Hepler, P.K. and Lord, E.M. (1998) Effects of Yariv phenylglycoside on cell wall assembly in the lily pollen tube. *Planta* 204: 450-458.
Seguí-Simarro, J.M. (2015) High Pressure Freezing and Freeze Substitution of *in Vivo* and *in vitro* Cultured Plant Samples. In *Plant Microtechniques: Methods and Protocols*. Edited by Yeung, E.C.T., Stasolla, C., Sumner, M.J. and Huang, B.Q. pp. 117-134. Springer International Publishing, Switzerland.
Seifert, G.J. and Roberts, K. (2007) The biology of arabinogalactan proteins. *Ann. Rev. Plant. Biol.* 58: 137-161.
Shibaya, T. and Sugawara, Y. (2009) Induction of multinucleation by β-glucosyl Yariv reagent in regenerated cells from *Marchantia polymorpha* protoplasts and involvement of arabinogalactan proteins in cell plate formation. *Planta* 230: 581-588.
Sitte, P. (1953) Untersuchungen zur submikroskopischen morphologie der pollen und sporoenmembranen. *Microskopie* 8: 290-299.
Southworth, D. and Kwiatkowski, S. (1996) Arabinogalactan proteins at the cell surface of *Brassica* sperm and *Lilium* sperm and generative cells. *Sex. Plant. Reprod.* 9: 269-272.
Stacey, N.J., Roberts, K., Carpita, N.C., Wells, B. and McCann, M.C. (1995) Dynamic changes in cell surface molecules are very early events in the differentiation of mesophyll cells from *Zinnia elegans* into tracheary elements. *The Plant Journal* 8: 891-906.

Tang, X.C., He, Y.Q., Wang, Y. and Sun, M.X. (2006) The role of arabinogalactan proteins binding to Yariv reagents in the initiation, cell developmental fate, and maintenance of microspore embryogenesis in *Brassica napus* L. cv. Topas. ***J. Exp. Bot.*** 57: 2639-2650.
Vaughn, K.C. (2003) Dodder hyphae invade the host: a structural and immunocytochemical characterization. *Protoplasma* 220: 189-200.
Vaughn, K.C., Talbot, M.J., Offler, C.E. and McCurdy, D.W. (2007) Wall Ingrowths in Epidermal Transfer Cells of Vicia faba Cotyledons are Modified Primary Walls Marked by Localized Accumulations of Arabinogalactan Proteins. *Plant Cell Physiol.* 48: 159-168.
Wilson, Z.A., Song, J., Taylor, B. and Yang, C. (2011) The final split: the regulation of anther dehiscence. ***J. Exp. Bot.*** 62: 1633-1649.
Willats, W.G., Steele-King, C.G., Marcus, S.E. and Knox, J.P. (1999) Side chains of pectic polysaccharides are regulated in relation to cell proliferation and cell differentiation. *Plant J.* 20: 619-628.
Willats, W.G.T., Limberg, G., Buchholt, H.C., van Alebeek, G.-J., Benen, J., Christensen, T.M.I.E., et al. (2000) Analysis of pectic epitopes recognised by hybridoma and phage display monoclonal antibodies using defined oligosaccharides, polysaccharides, and enzymatic degradation. *Carbohydrate Research* 327: 309-320.
Willats, W.G.T., Marcus, S.E. and Knox, J.P. (1998) Generation of a monoclonal antibody specific to (1→5)-α-l-arabinan. *Carbohydrate Research* 308: 149-152.
Willats, W.G.T., Orfila, C., Limberg, G., Buchholt, H.C., van Alebeek, G.-J.W.M., Voragen, A.G.J., et al. (2001) Modulation of the Degree and Pattern of Methyl-esterification of Pectic Homogalacturonan in Plant Cell Walls: Implications ofr pectic methyl esterase action, matrix proterties and cell adhesion. *Journal of Biological Chemistry* 276: 19404-19413.
Williams, M.A. (1977) Quantitative methods in biology (Practical methods in electron microscopy, vol 6, part 2). North Holland/American Elsevier, Amsterdam, The Netherlands.
Wiśniewska, E. and Majewska-Sawka, A. (2006) Cell wall polysaccharides in differentiating anthers and pistils of *Lolium perenne*. *Protoplasma* 228: 65-71.
Zhang, G.F. and Staehelin, L.A. (1992) Functional compartmentation of the Golgi apparatus of plant cells - Immunocytochemical analysis of high pressure frozen-substituted and freeze-substituted sycamore maple suspension culture cells. *Plant Physiol.* 99: 1070-1083.

Tables

Table 1: Antibodies used for immunolocalization

Primary antibody	Specificity	Provider	Dilution	Secondary antibody
AGPs				
JIM8	AGP	Carbosource, GA, USA	1:2	Goat anti-rat
JIM14	AGP	Carbosource, GA, USA	1:2	Goat anti-rat
JIM16	AGP	Carbosource, GA, USA	1:2	Goat anti-rat
JIM13	AGP	PlantProbes, Leeds, UK	1:5	Goat anti-rat
Pectins				
LM5	(1-4)-β-D-galactan	PlantProbes, Leeds, UK	undiluted	Goat anti- rat
LM6	(1-5)-α-L-arabinans	PlantProbes, Leeds, UK	undiluted	Goat anti- rat
JIM7	Highly methyl-esterified homogalacturonans	PlantProbes, Leeds, UK	1:2	Goat anti- rat
JIM5	Low methyl-esterified homogalacturonans	PlantProbes, Leeds, UK	1:2	Goat anti- rat
LM7	Partially methyl-esterified homogalacturonans	PlantProbes, Leeds, UK	undiluted	Goat anti- rat
Hemicelluloses				
CCRC-M1	Fucosylated xyloglucan	Carbosource, GA, USA	1:2	Goat anti-mouse
CCRC-M89	non-XXXG Xyloglucan	Carbosource, GA, USA	1:2	Goat anti-mouse
LM15	XXXG Xyloglucan	PlantProbes, Leeds, UK	undiluted	Goat anti- rat
LM11	Arabinoxylan and low-substituted xylan	PlantProbes, Leeds, UK	undiluted	Goat anti- rat

Legends to figures

Fig. 1: The different tissues of *B. napus* anthers during three developmental stages: 2.4 mm-long anthers (A-A''), 3.0 mm-long anthers (B-B'') and 3.7 mm-long anthers (C-C''). endo: endothecium; epi: epidermis; ls: locular space; mic: microspore; ml: middle layer; pg: pollen grain; tap: tapetum. Bars: A-C, A'-C': 10 µm; A''-C'': 5 µm.

Fig. 2: Quantification of AGP immunogold labeling with JIM18, JIM14 and JIM16 during anther development. For each subcellular region, different letters indicate significant differences among developmental stages. For each developmental stage, different numbers indicate significant differences among subcellular regions. Golgi+v: Golgi stacks + vesicles; Mid lam: middle lamella.

Fig. 3: Quantification of AGP immunogold labeling with JIM13 during anther development. For each subcellular region, different letters indicate significant differences among developmental stages. For each developmental stage, different numbers indicate significant differences among subcellular regions. Golgi+v: Golgi stacks + vesicles; Mid lam: middle lamella.

Fig. 4: Immunolocalization of JIM13 AGP epitopes. A, B: endothecium. In both 2.4 (A) and 3.7 mm-long anthers (B), JIM13 epitopes decorate the Golgi stacks (gs), from which they are delivered to the cell walls (cw). C, D: tapetum. In the tapetum of 2,4 mm-long anthers (C), JIM13 epitopes are being delivered to the locular space (ls) through vesicles (arrows), whereas these epitopes are dispersed through the cytoplasm of the degraded tapetal cells of 3.7 mm-long anthers (D). E: microspore of a 2.4 mm-long anther. F, G: pollen grain of a 3.7 mm-long anther. In E and F, gold particles only decorate the intine (in) and the locular space. In G, the labeling concentrates in the wall of the generative cell (gcw) separating the generative (gct) and vegetative cytoplasms (vct). ct: cytoplasm; er: endoplasmic reticulum; ex: exine; gn: generative nucleus; m: mitochondrion; v: vacuole. Bars: 500 nm.

Fig. 5: Quantification of pectin immunogold labeling with LM5, LM6, JIM7, JIM5 and LM7 during anther development. For each subcellular region, different letters indicate significant differences among developmental stages. For each developmental stage, different numbers indicate significant differences among subcellular regions. Golgi+v: Golgi stacks + vesicles; Mid lam: middle lamella.

Fig. 6: Immunolocalization of LM6 and JIM5 pectin epitopes in 2.4 mm-long anthers. A, B: endothecium. LM6 epitopes (A) are found in all cell wall (cw) regions, whereas JIM5 (B) epitopes concentrate in the middle lamella (ml). The arrow points to a cluster of JIM5 epitopes in a Golgi stack (gs). C: microspore showing LM6 labeling in the intine (in). D: pollen grain showing JIM5 labeling in the material deposited at the pollen surface (asterisk). ct: cytoplasm; er: endoplasmic reticulum; ex: exine; ls: locular space; v: vacuole. Bars: 500 nm.

Fig. 7: Quantification during anther development of xyloglucan immunogold labeling with CCRC-M1, CCRC-M89 and LM15, and of xylan immunogold labeling with LM11. For each subcellular region, different letters

indicate significant differences among developmental stages. For each developmental stage, different numbers indicate significant differences among subcellular regions. Golgi+v: Golgi stacks + vesicles; Mid lam: middle lamella.

Fig. 8: Immunolocalization of xyloglucan epitopes with CCRC-M1 (A, B) and xylan epitopes with LM11 (C, D) in 2.4 mm-long anthers. CCRC-M1 labeling decorates the cell walls (cw) of the endothecium layer (A), but it is absent from the intine (in) and the cytoplasm (ct) of microspores (B). LM11 epitopes are present in the cell walls of the endothecium (C), and in the pollen grains (D), where they decorate the intine and the material deposited at the pollen surface (asterisk). er: endoplasmic reticulum; ex: exine; ls: locular space. Bars: 500 nm.

Supplementary figures

Supplementary Fig. S1: Immunolocalization of AGP epitopes with JIM8 (A-C) and JIM14 (D-F) in 3.0 mm-long anthers. In the endothecium cell walls (cw) JIM8 labeling is almost absent, whereas in the tapetal cell walls (B), the pollen intine (in) and the locular space (ls) separating both cell types (C), JIM8 labeling is clearly observed. As to JIM14, labeling is very scarce in the endothecium (D), whereas tapetal cell walls (E), the locular space and the pollen intine (F) are clearly labeled. chl: chloroplast; chr: chromatin; er: endoplasmic reticulum; ex: exine; gs: Golgi stack; ls: locular space; m: mitochondrion; n: nucleus; ne: nuclear envelope; pm: plasma membrane; v: vacuole; ve: vesicle. Bars: 500 nm.

Supplementary Fig. S2: Immunolocalization of pectin epitopes with LM5 (A, B), JIM7 (C, D) and LM7 (E-F). A, B: LM5 immunolabeling in epidermal cells (A) and pollen grains (B) of 3.7 mm-long anthers. C, D: JIM7 immunolabeling in epidermal cells (C) and pollen grains (D) of 3.7 mm-long anthers. E, F: LM7 immunolabeling in endothecial cells of 2.4 mm-long (E) and 3.0 mm-long anthers (F). chl: chloroplast; er: endoplasmic reticulum; ex: exine; gs: Golgi stack; ls: locular space; m: mitochondrion; v: vacuole. Bars: 500 nm.

Supplementary Fig. S3: Immunolocalization of xyloglucan epitopes with CCRC-M89 (A, B) and LM15 (C, D) in 3.7 mm-long anthers. CCRC-M89 labeling decorates the cell walls (cw) but not the cuticle (cu) of epidermal cells (A), but it is very scarce in the intine (in) and the cytoplasm (ct) of microspores (B). LM15 epitopes are abundant in the cell walls but not the cuticle of epidermal cells (C), but very scarce in the intine and absent in the rest of the pollen grain (D). er: endoplasmic reticulum; ex: exine; ls: locular space. Bars: 500 nm.

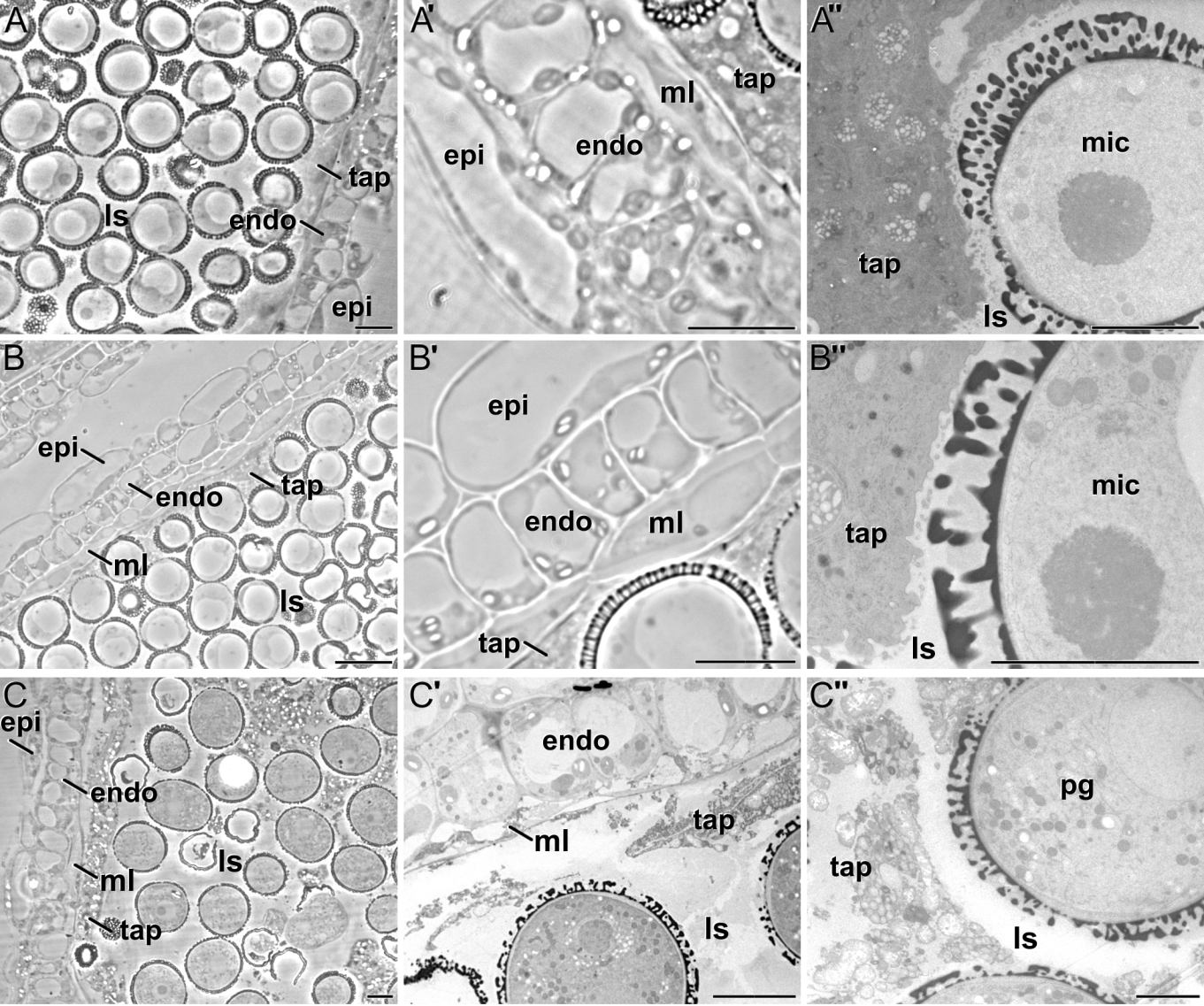
A
tap
ls
endo
epi
A'
ml
tap
epi
endo
A''
mic
tap
ls
B
epi
endo
tap
ml
ls
B'
epi
endo
ml
tap
B''
mic
tap
ls
C
epi
endo
ls
ml
tap
C'
endo
tap
ml
ls
C''
pg
tap
ls

Figure 1

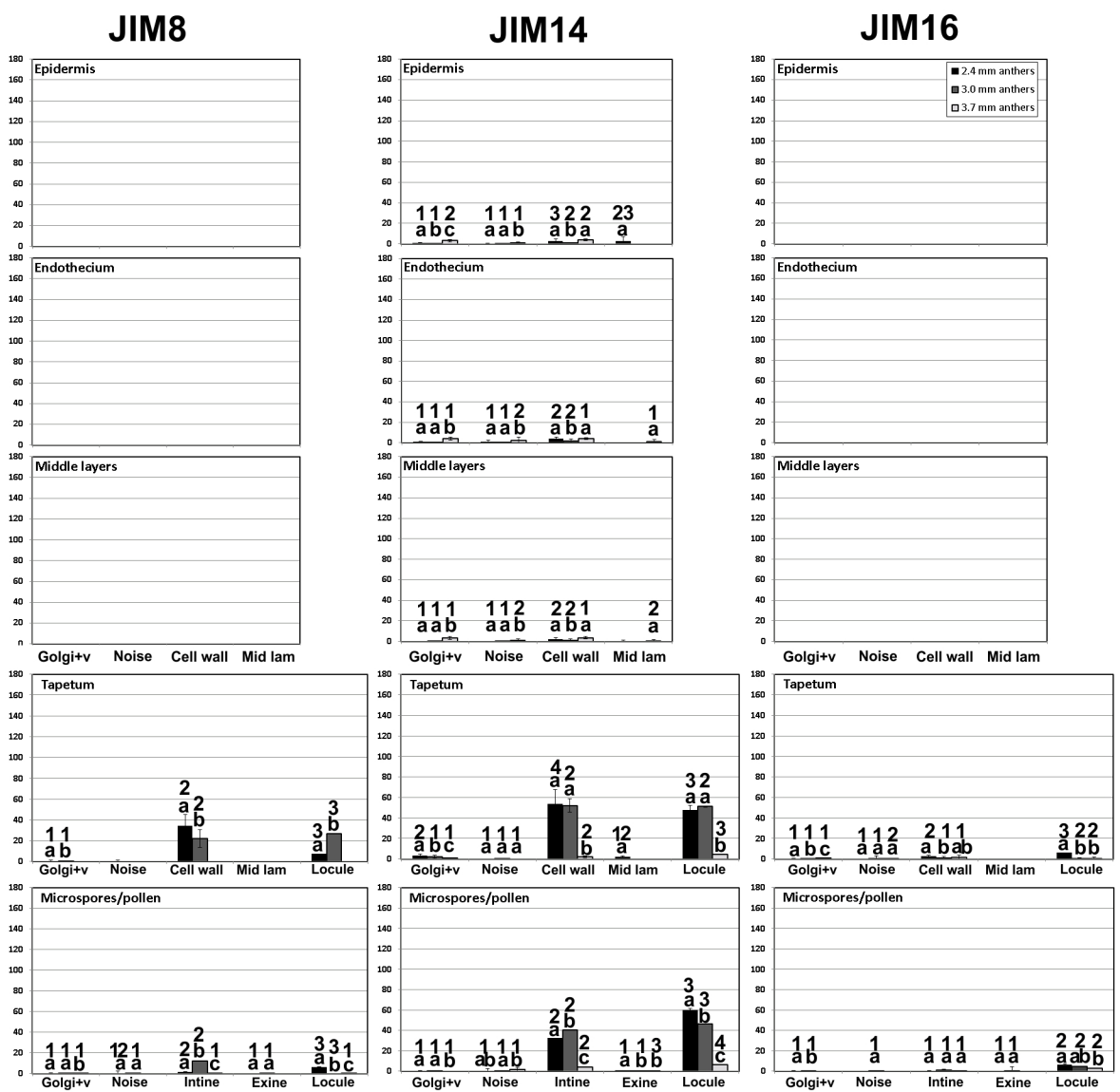
JIM8
JIM14
JIM16
Epidermis
Endothecium
Middle layers
Tapetum
Microspores/pollen
2.4 mm anthers
3.0 mm anthers
3.7 mm anthers
Golgi+v
Noise
Cell wall
Mid lam
Locule
Intine
Exine

Figure 2

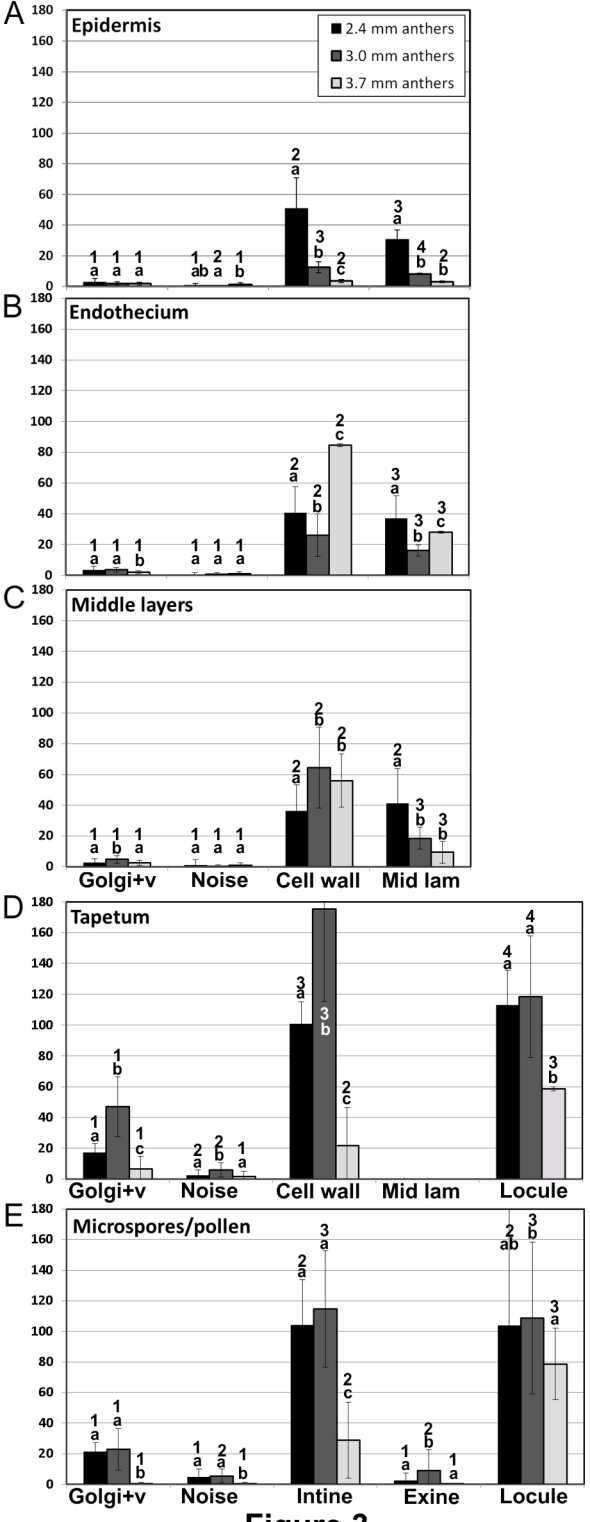
A
Epidermis
2.4 mm anthers
3.0 mm anthers
3.7 mm anthers
B
Endothecium
C
Middle layers
Golgi+v
Noise
Cell wall
Mid lam
D
Tapetum
Golgi+v
Noise
Cell wall
Mid lam
Locule
E
Microspores/pollen
Golgi+v
Noise
Intine
Exine
Locule

Figure 3

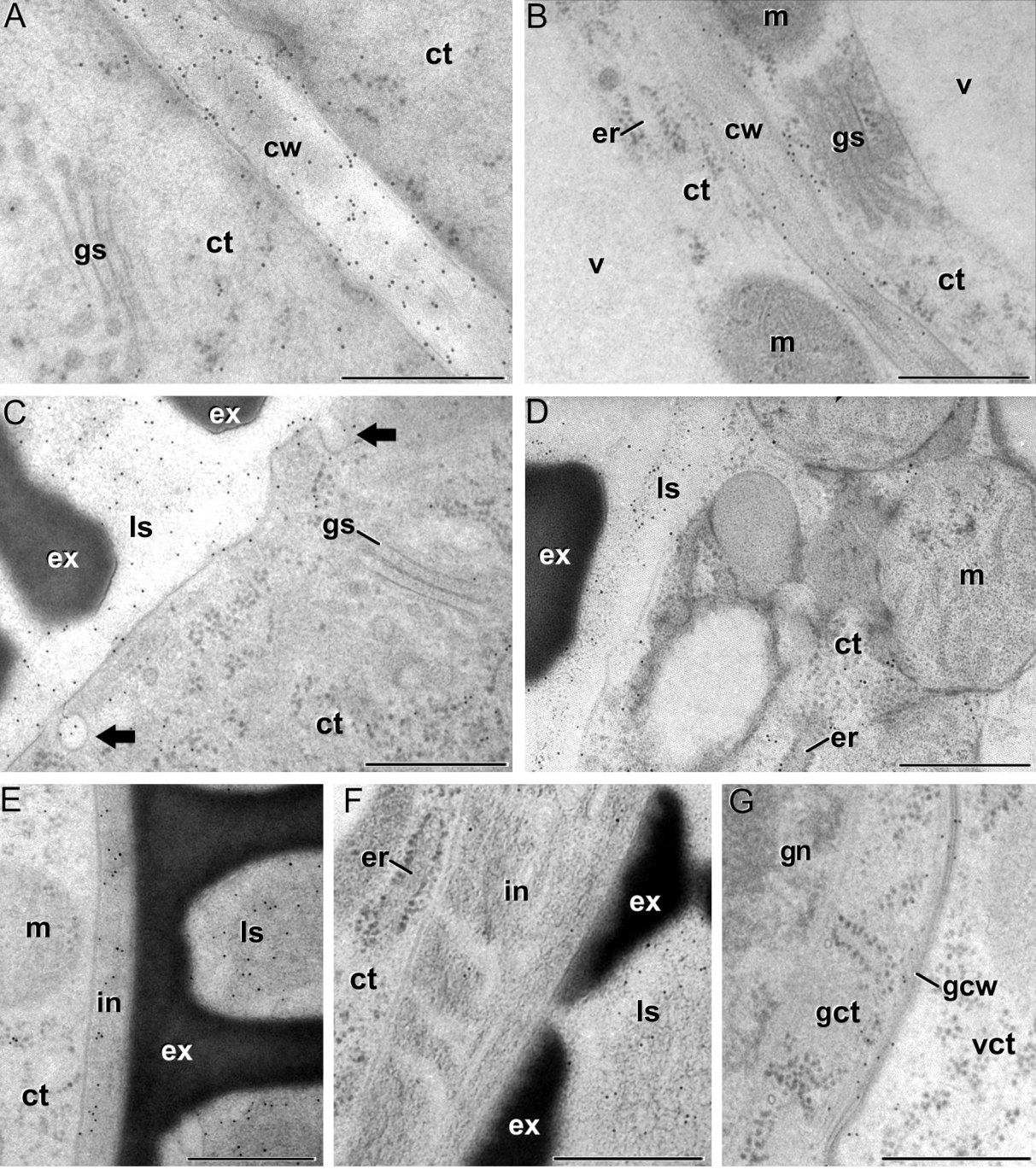
A
ct
cw
gs
ct
B
m
v
er
cw
gs
ct
v
ct
m
C
ex
ls
gs
ex
ct
D
ls
ex
m
ct
er
E
m
ls
in
ex
ct
F
er
in
ex
ct
ls
ex
G
gn
gcw
gct
vct

Figure 4

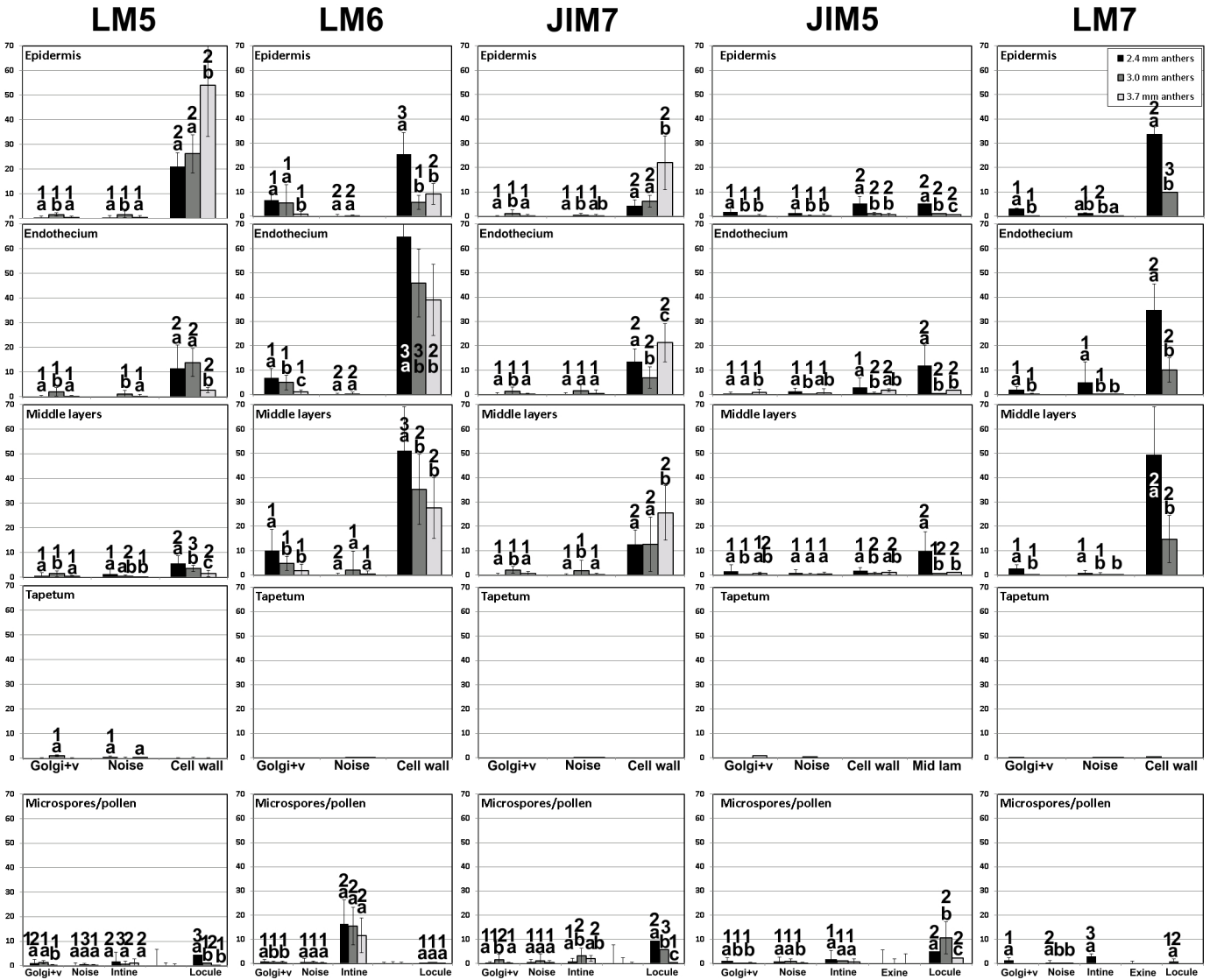
LM5
LM6
JIM7
JIM5
LM7
Epidermis
Endothecium
Middle layers
Tapetum
Microspores/pollen
2.4 mm anthers
3.0 mm anthers
3.7 mm anthers
Golgi+v
Noise
Cell wall
Mid lam
Intine
Exine
Locule

Figure 5

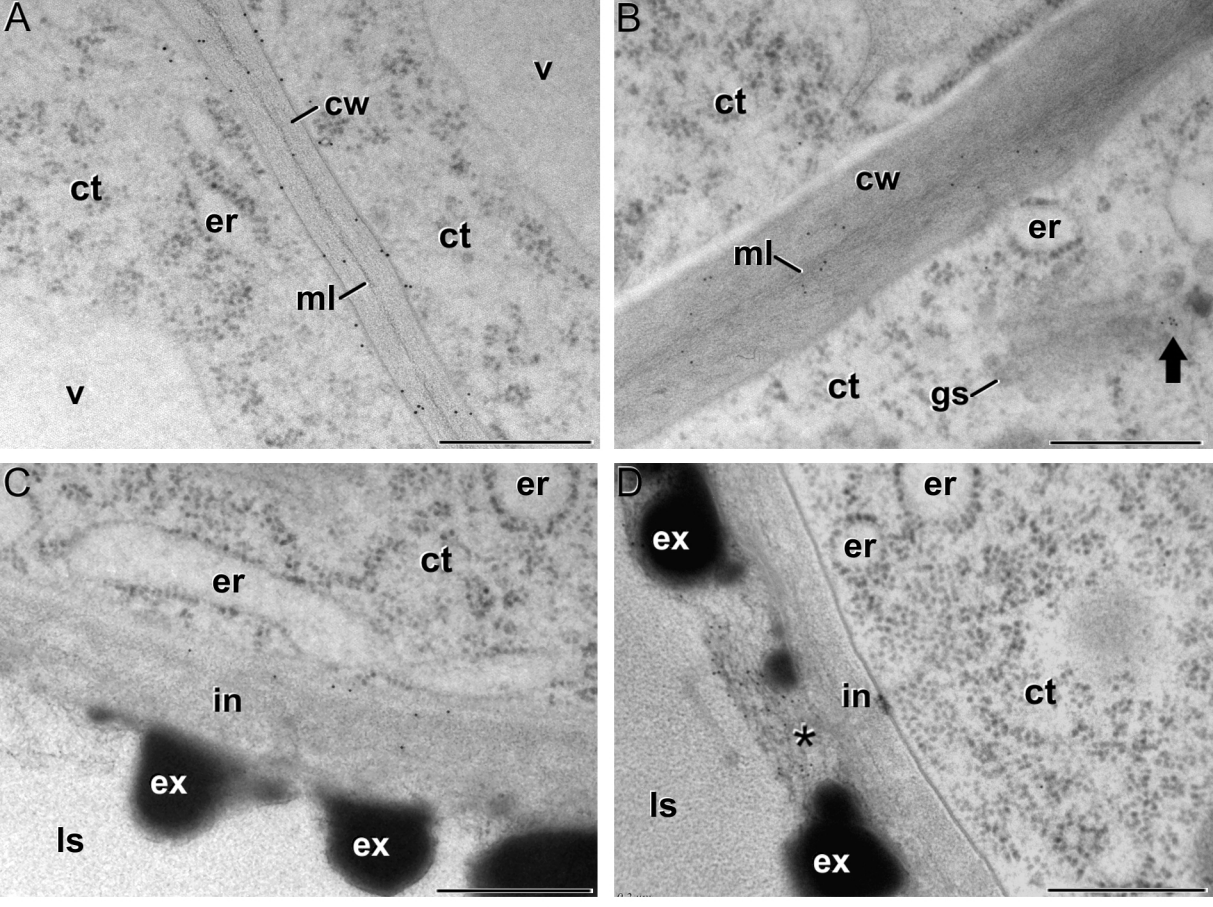
A
v
cw
ct
er
ct
ml
v
B
ct
cw
er
ml
ct
gs
C
er
er
ct
in
ex
ls
ex
D
er
ex
er
in
ct
*
ls
ex

Figure 6

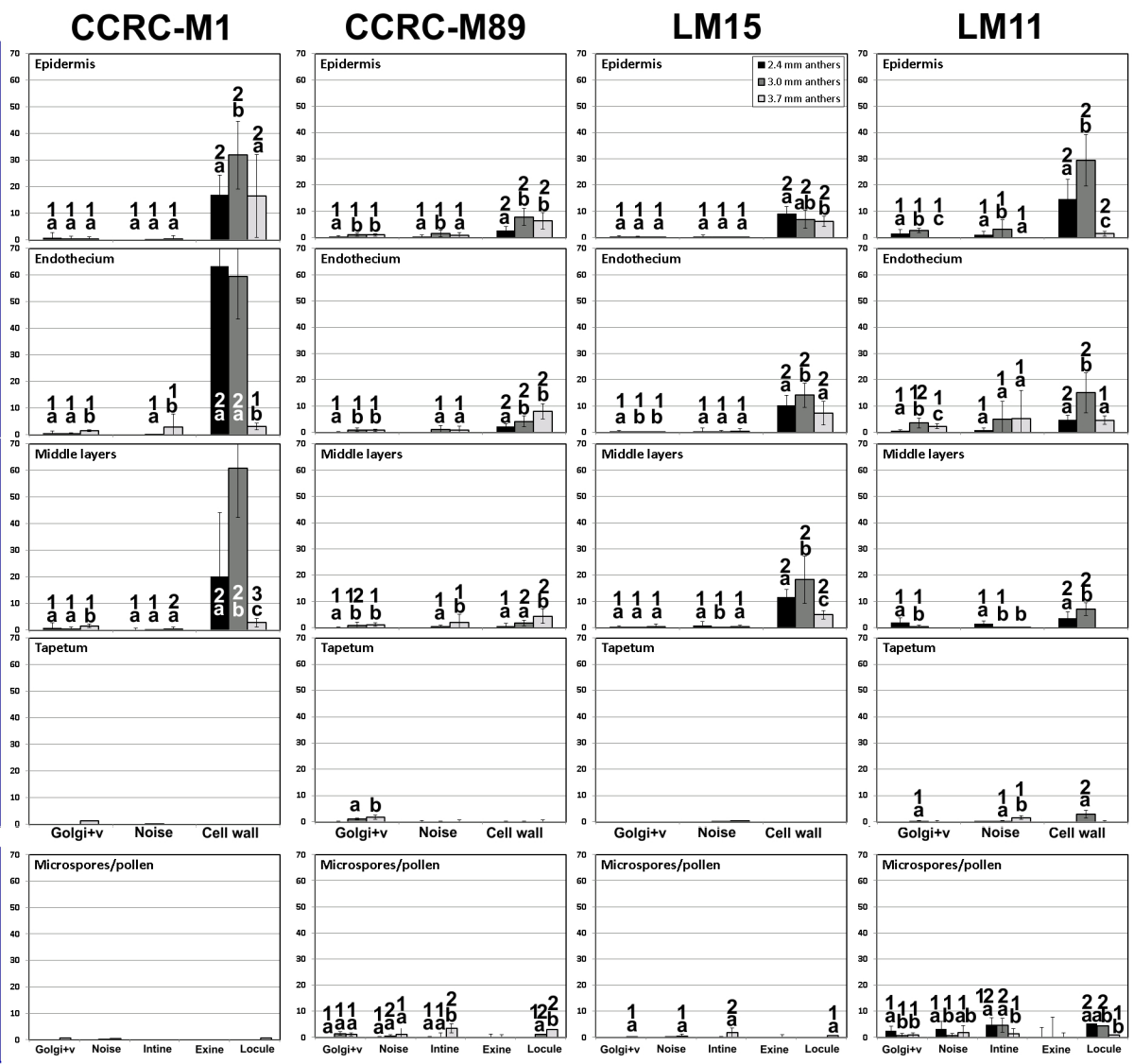
CCRC-M1
CCRC-M89
LM15
LM11
Epidermis
Endothecium
Middle layers
Tapetum
Microspores/pollen
2.4 mm anthers
3.0 mm anthers
3.7 mm anthers
Golgi+v
Noise
Cell wall
Intine
Exine
Locule

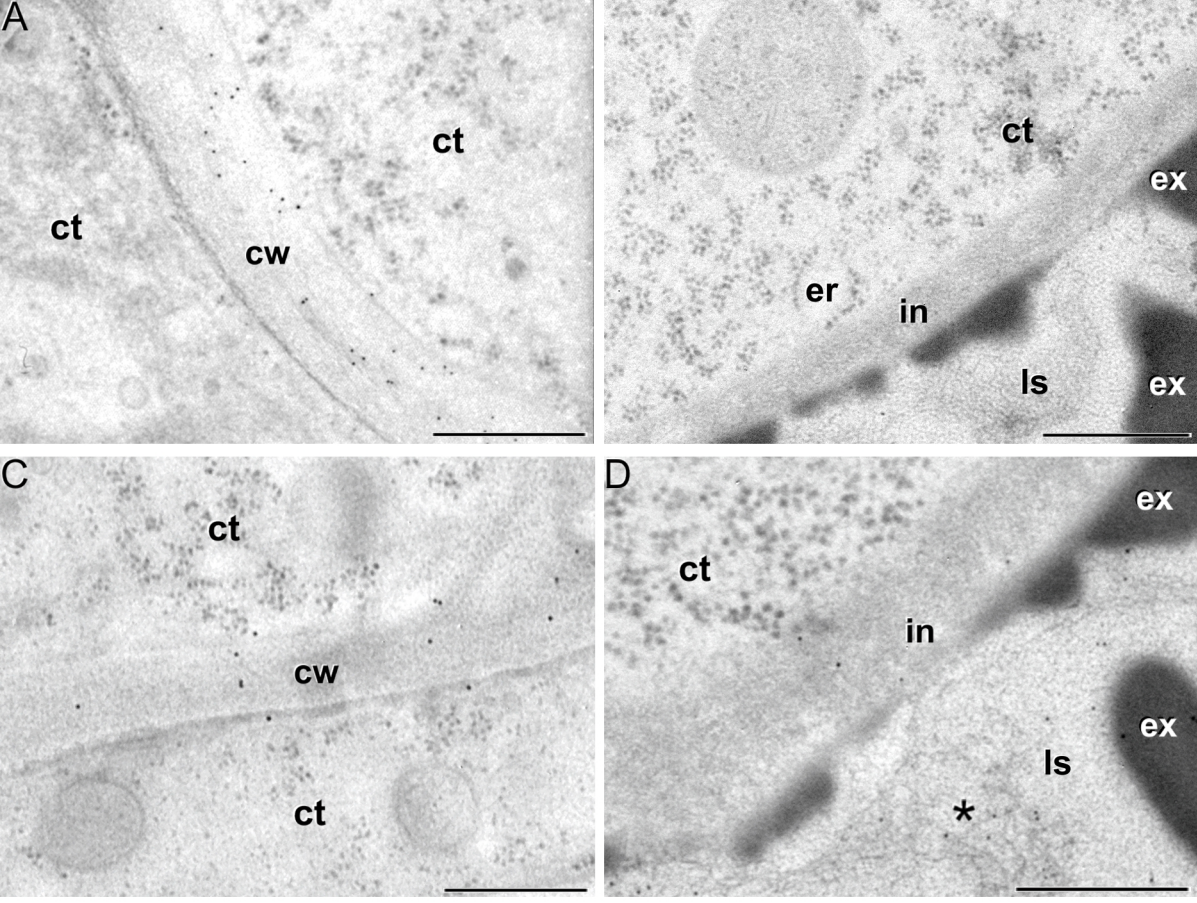

Figure 8

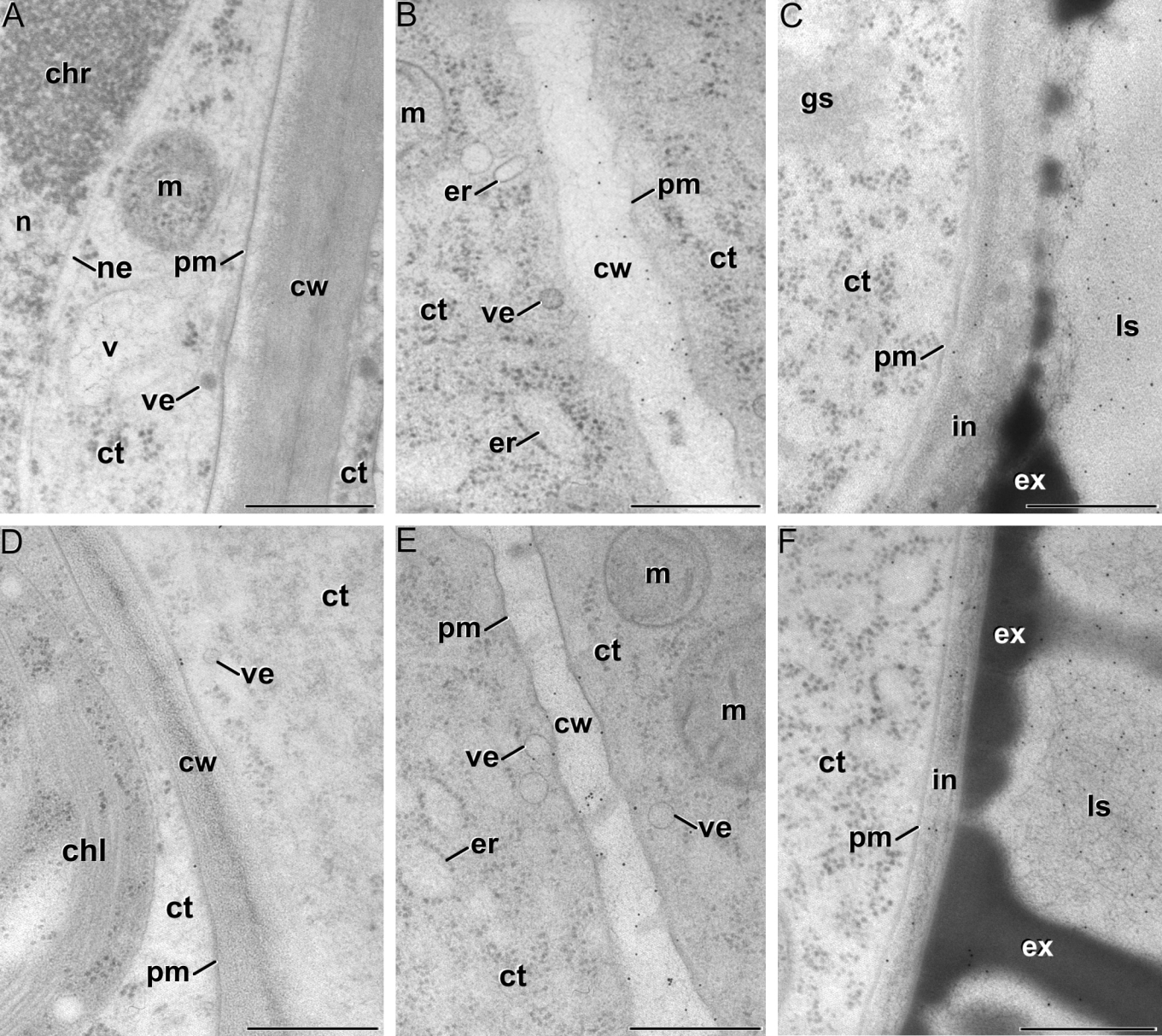
A
chr
m
n
ne
pm
cw
v
ve
ct
ct
B
m
er
pm
cw
ct
ct
ve
er
C
gs
ct
ls
pm
in
ex
D
ct
ve
cw
chl
ct
pm
E
m
pm
ct
cw
m
ve
ve
er
ct
F
ex
ct
in
ls
pm
ex

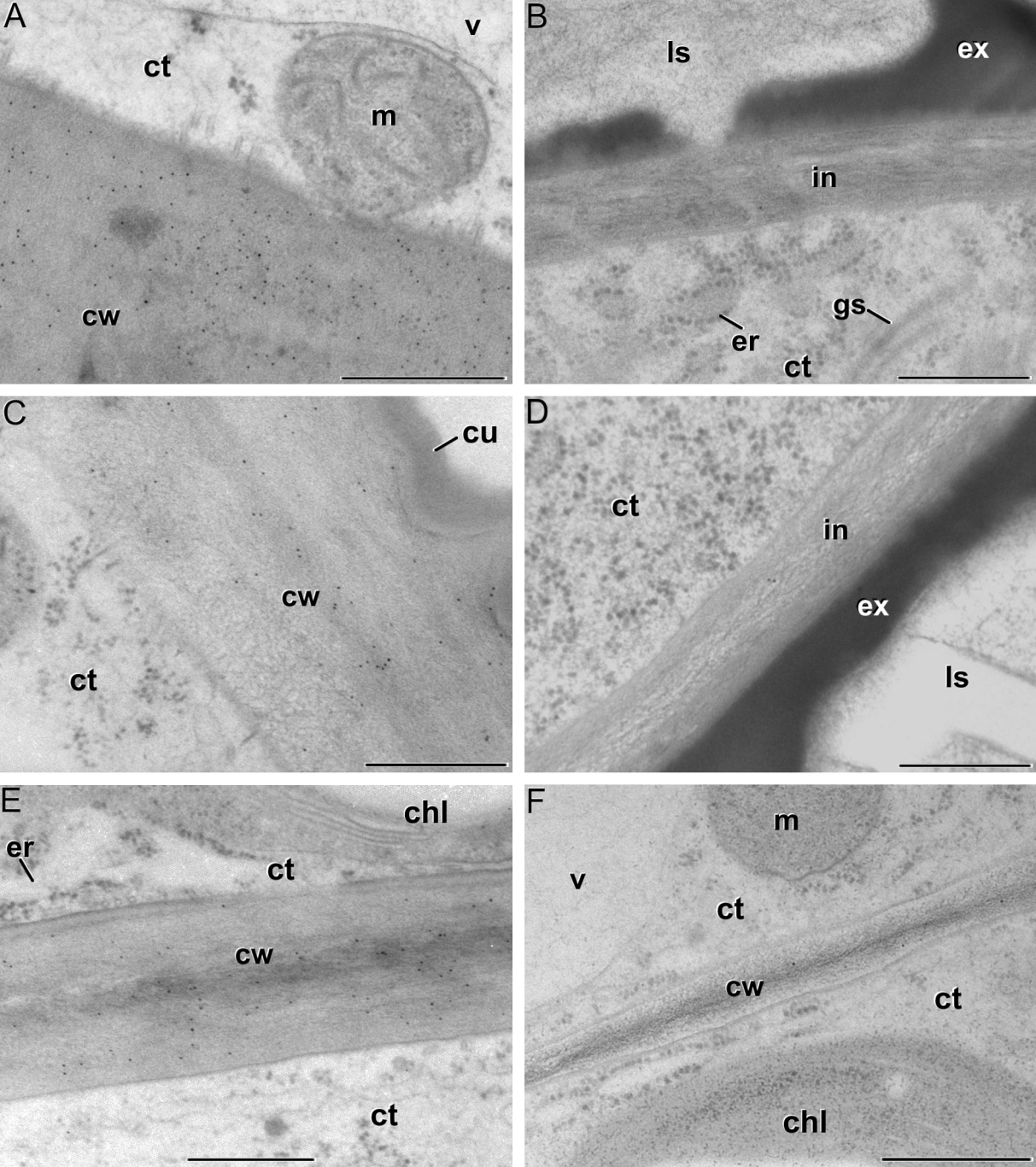
A
v
ct
m
cw
B
ls
ex
in
gs
er
ct
C
cu
cw
ct
D
ct
in
ex
ls
E
chl
er
ct
cw
ct
F
m
v
ct
cw
ct
chl

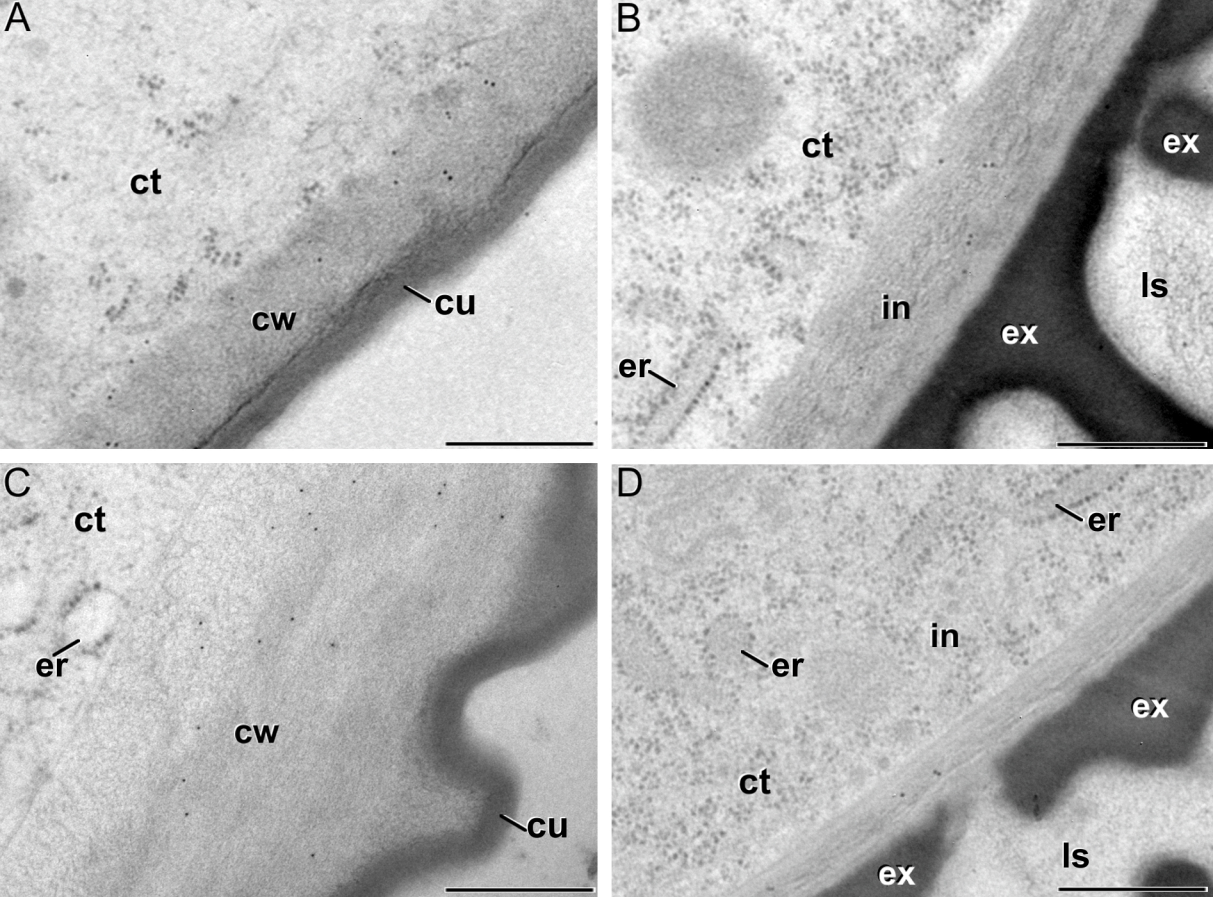
A
ct
cw
cu
B
ct
ex
ls
in
ex
er
C
ct
er
cw
cu
D
er
in
er
ex
ct
ex
ls